Supporting Online Material for

Entrainment of Neuronal Oscillations as a Mechanism of Attentional Selection

Peter Lakatos, George Karmos, Ashesh D. Mehta, Istvan Ulbert, Charles E. Schroeder*

*To whom correspondence should be addressed. E-mail: schrod@nki.rfmh.org

Published 4 April 2008, *Science* **320**, 110 (2008)
DOI: 10.1126/science.1154735

This PDF file includes:

Supporting Online Material

MATERIALS AND METHODS

Subjects. Electrophysiological data analyzed in this study were recorded in 24 penetrations of area V1 of the visual cortex in 2 male macaques (Macaca fascicularis, 11 and 13 penetrations per monkey). All procedures were approved in advance by the Animal Care and Use Committee of the Nathan Kline Institute.

Surgery. Preparation of subjects for chronic awake intracortical recording was performed using aseptic techniques, under general anesthesia. The tissue overlying the calvarium was resected and appropriate portions of the cranium were removed. The neocortex and overlying dura were left intact. To provide access to the brain and to promote an orderly pattern of sampling across the surface of visual areas, matrices of 18 gauge stainless steel guide tubes were positioned normal to the brain surface for orthogonal penetration of the lateral striate operculum, targeting the foveal representation of area V1. Implantation was guided by stereotaxic transformation of magnetic resonance imaging (MRI) data, which delineated the cortical gyral pattern. Individual epidural guide tubes were positioned over central and frontal sites to serve as ground and reference electrodes. Together with socketed Plexiglas bars (to permit painless head restraint), they were secured to the skull with orthopedic screws and embedded in dental acrylic. A recovery time of two weeks was allowed before the beginning of data collection.

Behavioral task and stimuli. The monkeys were trained to perform an intermodal selective attention task, which required them to attend to one modality, and discriminate stimuli within that same modality, while ignoring stimuli in the other modality. A trial block began when the monkey depressed a switch and fixated within a 1.5-degree window (Fig. 1). These events initiated a mixed stream of auditory and visual stimuli, and although the stimulus onset asynchrony was jittered within each modality (see below), the succession of different modality stimuli was kept constant. In each modality, 86 percent of the stimuli were standard, non-target stimuli, and 14 percent were deviant stimuli. The standard visual stimulus consisted of a 10 μs long, red light flash presented centrally and subtending 12 retinal degrees, and the deviant stimulus differed slightly in intensity. The auditory standard and deviant stimuli were pure tones that differed slightly in frequency. Stimuli were presented at a combined mean rate of about three per second: the stimulus onset asynchrony within one modality was between 500 and 800 ms (mean = 650 ms), while between auditory and visual stimuli it varied from 200 to 400 ms (mean = 300 ms). An infrared eye tracker monitored eye position at a resolution of approximately 1 retinal degree, and fixation within the 1.5 degree window had to be maintained throughout stimulus presentation. Selective attention was manipulated by requiring the monkey to release the switch in response to deviant stimuli in the attended modality alone. A cueing period preceding the trial block consisting of stimuli in just one modality instructed the monkey to attend to that modality during the following trial block. If the subject responded by switch release between 120 and 650 ms after presentation of the deviant stimulus in the appropriate modality, a drop of juice was delivered as reward. Deviants

could occur from the 2nd to the 10th position in the trials, and the trial ended following a correct response to the deviant in the attended modality. Reaction times were in the range of ~250–500 ms for visual discriminations and ~150–350 ms for auditory discriminations. Each trial block lasted 3-5 minutes with 40-60 target presentations, and selective attention to the visual and auditory modalities was tested alternating in successive trial blocks. Task difficulty was balanced across sensory modalities by altering the difference between the deviant and standard stimuli so that performance (as indexed by hits, misses, false alarms, and correct rejections) was maintained as close as possible to 90 percent correct. By equating the task difficulty across sensory modalities, arousal was maintained at comparable levels during the visual and auditory tasks. Presentation of all stimuli (auditory and visual) was gated by eye position, and only trials where subjects held their gaze within the eye position window for at least 1 s were analyzed. Animals performed for 2–4 h, yielding 10–20 trial blocks before indicating satiety.

Electrophysiology. Animals sat in a primate chair in a dark, isolated, electrically shielded, sound-attenuated chamber with head fixed in position. Laminar profiles of field potentials (EEG) and concomitant population action potentials (multiunit activity or MUA) were obtained using a linear array multi-contact electrode (14 contacts, 150 μm intercontact spacing). The multielectrode was inserted acutely through a guide tube sited above the area of interest for that session; it was lowered through the dura into the brain, and positioned with the electrode channels spanning all layers of the cortex (Fig. S1A). Posthumous histology confirmed most of the electrode positions. The impedance at each contact was

0.1~0.3 MΩ. Contacts were referenced to an epidural electrode at the frontal midline. Signals from each electrode contact were coupled via unity gain preamplifiers to Grass P5 and P12C amplifiers. For field potentials, signals were amplified with bandpasses of 3–500 Hz (Monkey 1), or 1–500 (Monkey 2). The phase shift introduced by the filters (High Pass: 6 dB/octave; Low pass: 12 dB/octave) was corrected offline (see data analysis). MUA was extracted from the same signals with a bandpass of 500-3000 Hz for MUA. MUA signals were rectified, 1000 Hz low pass filtered and resampled at 2000 Hz using custom hardware circuitry to extract an estimate of ensemble cell firing. The resulting field potential and MUA were then digitized at 2000 Hz sampling rate with a PC-based data acquisition system, and were stored as continuous records.

Data analysis. Data were analyzed offline using Matlab. Only stimulus trains associated with a correct behavioral response to the deviant in the attended modality were analyzed. One-dimensional CSD profiles were calculated from field potential profiles using a three-point formula to estimate the second spatial derivative of voltage (*S1*). CSD profiles provide an index of the location, direction, and density of transmembrane current flow, the first-order neuronal response to synaptic input (*S2*). Also, using the standard red flash related laminar CSD profile and the average spatial dimensions of the cortical layers, the functional identification of supragranular, granular and infragranular cortical layers in area V1 is straightforward based on our earlier studies (*S2*).

To extract visual event related response amplitudes, we calculated the analytic amplitude of the single trial CSD signals for the entire pass-band using the Hilbert

transform, and both the CSD amplitude and MUA signals were baseline corrected over the -100–0 ms pre-stimulus time interval (Fig. S1A). In the present study we excluded the first standard of each stimulus train from the analysis, because we were interested in attention effects related to the temporal structure of the task; this could not be established until at least 2 stimuli had occurred. To quantify response amplitude differences between attend visual (AV) and attend auditory (AA) conditions, we averaged the single trial analytic CSD amplitude and the MUA across all trials and layers within experiments, and pooled the cross-laminar CSD and MUA waveforms across all experiments (Fig. S1B). Statistical analysis of pooled visual response amplitudes (n = 24) in the post-stimulus interval (Fig. S1B, bottom traces) revealed significant response enhancement in the ~15-200 ms time-frame for CSD, and in the ~50-135 ms time-frame for MUA in the AV condition (Wilcoxon signed rank, $p < 0.01$). Comparison of response amplitudes within each experiment, based on single trial CSD and MUA responses across all layers in the 50-135 ms time interval revealed a significantly larger response in the AV compared to the AA condition in each of the recording sites (Wilcoxon rank sum, $p < 0.01$); on average, CSD response amplitude (Fig. S1C) was 62% percent larger (range = 27-105%; standard deviation (SD) = 24; n = 24), and MUA amplitude was 46% larger (range = 16-84 %; SD = 18; n = 24) in the AV compared to the AA condition. Note that CSD amplitude differences start before the earliest visual response onset in V1 (mean = 33.5 ms; SD = 4.1 ms; n = 24), which indicates attentional modulation of the baseline or pre-stimulus activity. This early CSD amplitude difference is related to entrainment rather than stimulus related response, since it is a consequence of increasing (attend visual) and decreasing (attend auditory)

CSD "amplitude trends", which start before the presentation of visual stimuli (Figs. S1A and S2B).

To characterize signed pre-stimulus CSD amplitudes in different cortical layers the AV and AA conditions we averaged single trial non-baseline corrected CSD in the -100 to 0 ms time interval on selected supra- granular and infragranular electrodes within each individual experiment. Electrodes were selected based on largest visual stimulus related response in all layers. We found that supragranular baseline CSD activity was opposite in sign, and it was significantly different in all of our experiments in the two attention conditions ($n = 24$, Wilcoxon rank sum, $p < 0.05$). The same was true for infragranular layers for most of our recordings (significant in 14 out of 24, Wilcoxon rank sum, $p < 0.05$). On the contrary, granular layer pre-stimulus CSD activity had the same sing (sink) in all of our experiments, and it differed significantly only in 3 cases. These data show that while the temporal pattern of granular layer CSD activity is dominated by periodic visual responses (qualitatively similar across attention conditions), the corresponding pattern in the extragranular laminae is dominated by attention, and is thus 180 degrees out of phase in the AA and AV conditions (Fig. S2).

To examine the laminar amplitude profile of pre-stimulus oscillations, we calculated the analytic amplitude (Hilbert transform) of the pre-stimulus (-100–0) CSD for the entire pass-band. The pre-stimulus CSD amplitude (graph between CSD profiles in Fig. 2A) was largest in the supragranular layers in all of our V1 recordings (Games-Howell test, $p < 0.01$). Earlier observations indicate that the pre-stimulus oscillations of the supragranular layers play a key role in modulating the event related response (*S3*,*S4*), and

that these layers display maximal attentional modulation in V1 (*S5*). Thus, we selected the supragranular site with the largest pre-stimulus activity and initial event related activation (current sink) for the analysis of pre-stimulus oscillations.

Continuous recordings were epoched off-line from -2000 to 2000 ms to avoid edge effects of the wavelet transformation using standard visual (Figs. 2-3 and related analysis), standard auditory (analysis of delta inter-trial coherence) or deviant visual stimuli (Fig. 4 and related analysis) as triggers. Instantaneous power and phase were extracted by wavelet decomposition on 84 scales from 1 to 101.2 Hz (Morlet wavelet (*S6*)).

We decided to analyze pre-stimulus gamma amplitude, because previous studies have found that attention results in enhanced gamma coherence (*S7*,*S8*). The mean frequency of pre-stimulus gamma oscillations averaged in the -50 to 0 ms time window in the wavelet transformed data was 43.5 Hz (SD = 5.1) in the 24 experimental sessions comprising this study. After determining the peak frequency for each experiment, gamma amplitude was averaged in a 20 Hz frequency window centered on this for each single trial. Pre-stimulus gamma amplitude was on average 9.3 percent larger (SD = 4.3; n = 24) in the AV than in the AA condition (Fig. 2G), and this increase was statistically significant in 21 out of 24 experiments (Wilcoxon rank sum, $p < 0.05$). In contrast, at -325 to -275 ms pre-stimulus, gamma amplitude was on average 7.4 percent smaller (SD = 3.7; n = 24) in the AV condition; in 17 out of 24 cases this difference proved to be significant on the single trial level (Wilcoxon rank sum, $p < 0.05$).

To characterize entrained pre-stimulus delta phase distribution across trials, we analyzed phase values at visual stimulus onset (0 ms) and at the frequency corresponding

to the mean stimulus presentation frequency within one modality (~1.5 Hz). Since the analog filters used in the present experiments cause a considerable amount of phase distortion, we calculated the phase shift introduced by the 3 Hz (Monkey 1) and 1 Hz (Monkey 2) high-pass filters (6 dB/octave) at 1.5 Hz (1.02 rad, and 0.52 rad, respectively), and corrected the phase values. After determining that phase distributions were non-uniform in both conditions in all experiments using Rayleigh's uniformity tests ($p < 0.01$), we calculated the mean phases (AV: ϕ mean = 2.7 rad, ϕ dev = 0.61, n = 24; AA: mean = 0.23 rad, ϕ dev = 0.87, n = 24). Phase distributions were compared by a nonparametric test for the equality of circular means (*S9*), and we found that the phase difference between AV and AA conditions was significant ($p < 0.01$), delta oscillation was in counter-phase in the two attention conditions.

To determine whether visual stimuli alone orchestrate the counter-phase entrainment of delta oscillations, we compared delta inter-trial coherence ITC) related to visual and auditory stimuli in the two attention conditions. ITC ranges from 0 to 1; higher values indicate that the observations (phase at a given frequency and time-point across trials) are clustered more closely around the mean angle than lower values. ITC is larger in the case of stimuli that re-set, and thus entrain delta oscillations. We calculated the difference between attention conditions 50 ms post-stimulus at 1.5 Hz using both visual and auditory stimuli, and we found that the ITC was larger in the case of visual stimuli in the AV condition, (AV-AA ITC was positive: mean = 0.13; SD = 0.05), while it was larger in the case of auditory stimuli in the AA condition (AV-AA ITC was negative: mean = -0.12; SD = 0.05) in all of our experiments (n = 24). Since ITC is dependent on the sample

size, and the number of trials was somewhat variable across different experiments/experimental conditions, we tested whether these attention-related delta ITC differences were statistically significant within each of the 24 V1 recordings using the non-parametric statistical method proposed by Maris et al. (*S10*), which is independent of unequal sample sizes. The AV-AA ITC difference proved to be significant in 22 out of 24 experiments in the case of visual, and 20 out of 24 experiments in the case of auditory events (Monte Carlo $p < 0.05$).

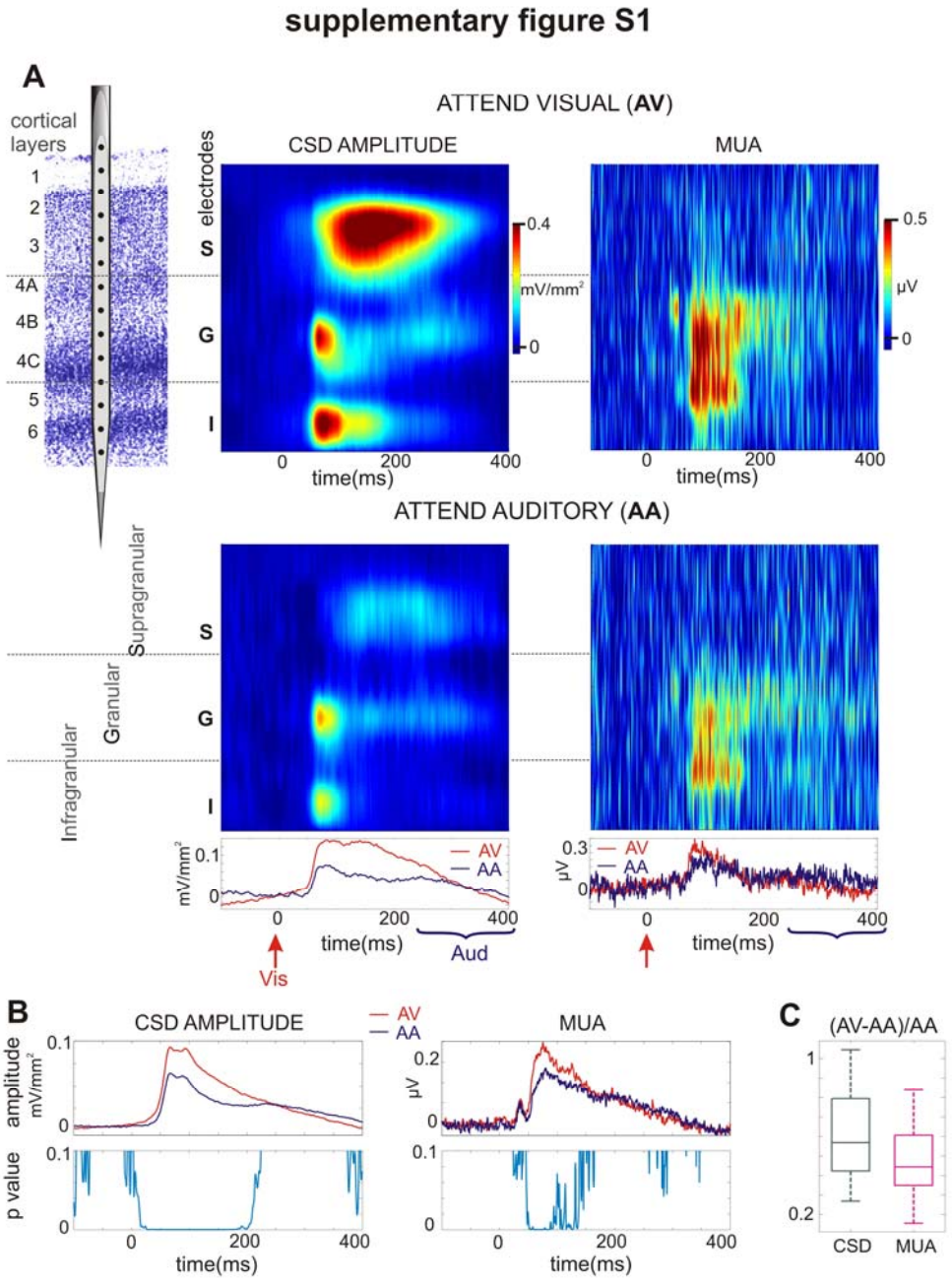

Fig. S1. *The effect of attention on visual event related responses in area V1*. **(A)** Color-maps show the laminar profiles of standard visual stimulus related averaged and baseline corrected single trial CSD amplitudes (analytic amplitude) and MUA in the AV and AA

conditions with data combined across a representative recording session (562 and 519 single trials respectively). Traces below the color-maps show the time course of CSD amplitude and MUA averaged across all layers. Red arrow below the time axis indicates the time of the visual event used as trigger, while blue bracket indicates the time-frame where auditory events could occur relative to the visual event; since SOA was variable over trials, onset time is 'smeared' over time for all stimuli except that used as a trigger for signal averaging. (**B)** Above: time course of standard visual event related laminar CSD amplitude and MUA averaged across both subjects and all recordings (n=24) in AV and AA conditions. Traces below show p values (Wilcoxon signed rank) derived from statistically comparing CSD and MUA amplitudes in the AV vs. AA conditions. (**C)** Pooled normalized CSD and MUA response amplitude differences between AV and AA conditions ([AV-AA]/AA) in the 50-135 ms time-interval. The boxes have lines at the lower quartile, median, and upper quartile values.

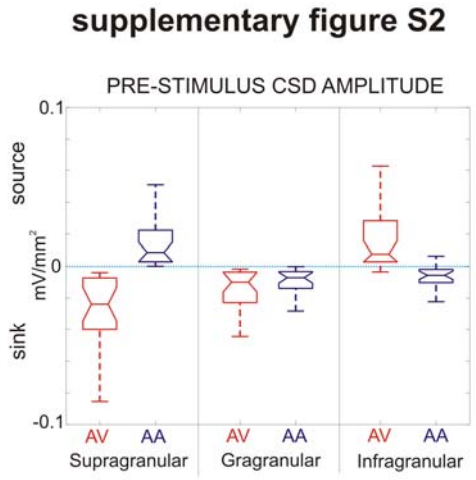

Fig. S2. *The effect of attention on pre-stimulus CSD sign and amplitude in different cortical layers.* Box-plots show pre-stimulus (-100 - 0 ms) CSD sign (i.e., source or sink) and amplitude in selected supragranular, granular, and infragranular channels in the AV and AA conditions for all experiments (n=24). Note that while pooled supragranular and infragranular CSD amplitudes are opposite in sign in the two attention conditions, granular pre-stimulus CSD sign is the same (sink) across conditions.

REFERENCES FOR SUPPORTING ONLINE MATERIAL

S1. C. Nicholson, J. A. Freeman, *J. Neurophysiol.* **38**, 356 (1975).

S2. C. E. Schroeder, A. D. Mehta, S. J. Givre, *Cereb. Cortex* **8**, 575 (1998).

S3. P. Lakatos *et al.*, *J. Neurophysiol.* **94**, 1904 (2005).

S4. P. Lakatos, C. M. Chen, M. N. O'Connell, A. Mills, C. E. Schroeder, *Neuron* **53**, 279 (2007).

S5. A. D. Mehta, I. Ulbert, C. E. Schroeder, *Cereb. Cortex* **10**, 343 (2000).

S6. C. Tallon-Baudry, O. Bertrand, C. Delpuech, J. Pernier, *J Neurosci.* **16**, 4240 (1996).

S7. P. Fries, J. H. Reynolds, A. E. Rorie, R. Desimone, *Science* **291**, 1560 (2001).

S8. T. Womelsdorf, P. Fries, P. P. Mitra, R. Desimone, *Nature* **439**, 733 (2006).

S9. D. S. Rizzuto, J. R. Madsen, E. B. Bromfield, A. Schulze-Bonhage, M. J. Kahana, *Neuroimage.* **31**, 1352 (2006).

S10. E. Maris, J. M. Schoffelen, P. Fries, *J. Neurosci. Methods* **163**, 161 (2007).